Mesomorphic polymorphism of binary mixtures of water and surfactants

A. Linhananta and D. E. Sullivan
Department of Physics and Guelph-Waterloo Program for Graduate Work in Physics, University of Guelph, Guelph, Ontario N1G 2W1, Canada

(Received 26 August 1997; revised manuscript received 18 December 1997)

In this work, a vector lattice model is employed to study binary mixtures of water and surfactants. The face-centered-cubic lattice is employed in order to best approximate a realistic liquid environment. The model is analyzed by low-temperature expansion and Monte Carlo methods. It is shown that for sufficiently strong surfactant-water interactions the system exhibits a rich polymorphism where up to eight phases are stable. In addition to the disordered water-rich and surfactant-rich phases, liquid-crystalline phases such as the hexagonal and the lamellar phases as well as the inverse bicontinuous cubic, inverse hexagonal and inverse micellar cubic phases are stable in the model. It is shown that the inverse bicontinuous cubic structure in our model is remarkably similar to the gyroid phase. The formation of water channels in the surfactant bilayers of a lamellar phase is also examined. [S1063-651X(98)13104-5]

PACS number(s): 64.70.Ja, 64.60.Cn, 05.50.+q, 87.15.Da

I. INTRODUCTION

Binary mixtures of water and surfactants exhibit a rich polymorphism due to their tendency to form water-surfactant interfaces. At low surfactant concentration, surfactant molecules form aggregates or micelles that shield their hydrocarbon tails from water, leaving only their polar heads exposed. Depending on the chemical properties of the surfactant and the temperature of the system, the micelles usually assume a dominant geometrical shape which can be spherical, cylindrical, or a two-dimensional bilayer. At higher concentration and sufficiently low temperature, these micelles are the basic building blocks for a rich array of complex liquid-crystalline phases. For example, spherical or finite cylindrical micelles give rise to micellar cubic (Q'') phases which consist of periodic arrangements of these micelles. With increasing concentration, the hexagonal (H), bicontinuous cubic (Q'), and lamellar (L_α) phases, in that order, are observed to be stable. As is well known, the lamellar phase is a one-dimensionally ordered stack of infinite surfactant bilayers, whereas the hexagonal phase consists of infinite cylindrical micelles arranged in a two-dimensional array. For the latter phase, the two-dimensional array is either hexagonal or distorted hexagonal. The bicontinuous cubic phase, which is intermediate between the hexagonal and the lamellar phases, is a three-dimensional periodic arrangement where both the water and surfactant form continuous networks that span the system. At surfactant volume fractions that are significantly higher than 0.5, the inverse analogs of the above-mentioned phases are expected to be stable. These are the inverse bicontinuous cubic (IQ'), the inverse hexagonal (IH), and the inverse micellar cubic (IQ'') phases.

Experimentally, most surfactant-water mixtures do exhibit the above-mentioned universal phase behavior. However, the chemical properties of surfactant molecules can also give rise to very specific features. For example, the micellar cubic (Q'') phase is usually observed in mixtures containing cationic surfactants [1] or nonionic surfactants with bulky head groups [2]. Similarly, in mixtures containing anionic surfactants or surfactants with very long tails, the Q' phase is not stable but is replaced by an intermediate lamellar [3] phase in which each surfactant bilayer is pierced by water-filled channels. For some systems the water channels are arranged in a two-dimensional array, whereas in others the arrangements are random. There are also systems in which, in addition to the two-dimensional order of the channels, there is also a correlation between channels in adjacent bilayers, resulting in a tetragonal arrangement of water channels. Another example of nonuniversal behavior is that, in mixtures where the tail groups of the surfactants are especially bulky (such as phosolipids), the phase diagrams are dominated by inverse phases [4]. Similar universal and specific behavior is also observed in mixtures of *A*-*B* diblock copolymer and *A* or *B* homopolymer [5,6]. These systems show the same progression of stable phases from the disordered micellar phase to the ordered micellar cubic, hexagonal, bicontinuous cubic, and lamellar phases when a composition variable such as the concentration of added homopolymer is varied. This similarity is explained by the fact that copolymer-homopolymer and water-surfactant mixtures both tend to form interfaces between two distinct fluid components.

At a given surfactant concentration, the mixture organizes into a phase consisting of water-surfactant interfaces. The configuration of the phase is determined by the competition between interaggregate and intra-aggregate forces between surfactant molecules. The interaggregate forces favor flat interfaces, whereas intra-aggregate forces tend to favor curved interfaces. By employing topological arguments, Charvolin and Sadoc [7] showed that this interfacial ''frustration'' results in the formation of the various mesophases observed in binary mixtures of water and surfactants, confirming that the phase behavior of these systems is due mainly to the amphiphillic nature of surfactants. However, they did not consider the energetics associated with these interactions. In general, the free energy of the mixture is a function of the temperature, surfactant concentration, and curvature of the surfactant-water interface. At a fixed temperature and concentration, the free energy is minimized when the curvature assumes a value equal to the spontaneous curvature of the mixture [8]. The spontaneous curvature is the preferred cur-

vature of the interface, and is determined by the chemical properties of the surfactant molecules. For example, in mixtures containing ionic surfactants, the electrostatic repulsions between surfactant head groups result in spontaneous curvatures that are favorable to the formation of high curvature phases such as the Q'' and H phases [9]. For such mixtures, a stable lamellar phase is induced by increasing the surfactant concentration or by the addition of ionic salt which screens the head group repulsions [10]. Mixtures containing surfactants with long alkyl tails favor the formation of flat interfaces resulting in phase diagrams dominated by the lamellar phase. In mixtures containing surfactants with bulky tails, steric interactions between the tail groups favor the formation of surfactant-water interfaces that are concave with respect to the water regions resulting in phase diagrams dominated by inverse phases [4].

This paper focuses on the universal properties of binary mixtures of water and surfactants. Due to the complexity of water-surfactant mixtures, most theoretical models that examine these properties are either phenomenological or lattice models. A Ginzburg-Landau model with a scalar field and a vector field was employed by Gompper and Klein [11] to obtain a phase diagram with the above-mentioned phase sequence. Dawson and Kurtovic [12] applied ground-state and mean-field analyses to a vector lattice model, and obtained a phase sequence of lamellar, cylindrical, and cubic phases. The present work employs a vector lattice model similar to that of Ref. [12] and to that used by Matsen and Sullivan [13], Laradji *et al.* [14] and Ciach and co-workers [15], in their studies of tenary mixtures of water, oil, and surfactants. The model, which is presented in Sec. II, generalizes the two-component lattice gas model by allowing the component representing a surfactant molecule to have a discrete orientation. To best represent a realistic liquid environment, the model is studied on a face-centered-cubic (fcc) lattice. Although the model contains universal features that are common to all surfactant-water mixtures—mainly their ability to form interfaces—it does not contain nonuniversal features that are associated with the chemical structures of surfactants. This means that the model can be employed to identify and understand the universal behaviors of binary mixtures of water and surfactants. The goal of this study is similar to a recent Monte Carlo study of a lattice model by Larson [16]. However, the simple form of our model permits it to be analyzed by a variety of methods. The simplicity of the analyses clarifies the physics that underlines the mesomorphic polymorphism of binary water-surfactant mixtures.

In Sec. III ground-state and low-temperature analyses of the model are presented. It is found that for sufficiently strong surfactant-water interaction, with increasing surfactant chemical potential, the phase sequence W, H, L_α, IQ', IH, IQ'', and S phases, in that order, is observed to be stable. The W and S phases are disordered water-rich and surfactant-rich phases, respectively. Also examined is the formation of water channels in surfactant bilayers of a stable lamellar phase. In Sec. IV phase diagrams obtained by the low-temperature expansion method are presented. These results are compared with Monte Carlo simulation data to be presented more fully in a subsequent paper [17]. Finally, a discussion of the results and a summary are presented in Sec. V.

II. MODEL

In the lattice model employed in this work, the surfactant and water molecules are restricted to occupying a face-centered-cubic lattice. As in the Ising lattice gas model, each lattice site u is assigned a spin variable σ_u, which takes a value $+1$ or 0 to represent a water molecule or a surfactant molecule, respectively. In addition, a vector variable $\hat{s}$ is assigned to every surfactant molecule to describe its orientational degrees of freedom. In this work the orientation of a surfactant occupying a site u is restricted to point toward one of its 12 nearest neighbors. The Hamiltonian is

$$H=-\sum_{\langle u,v\rangle}\left[J_1\sigma_u\sigma_v+J_2(\sigma_v\hat{s}_u\cdot\hat{r}_{uv}+\sigma_u\hat{s}_v\cdot\hat{r}_{vu})\right]$$

$$-\mu_s\sum_u(1-\sigma_u), \tag{1}$$

where $\langle u,v\rangle$ denotes a summation over all distinct pairs of nearest neighbor sites u and v. The vector $\hat{r}_{uv}$ specifies the direction from lattice site u to site v. For convenience we set $|\hat{r}_{uv}|=1$, where the length scale is in units of the lattice spacing. The term with coupling J_1 represents the isotropic interactions between nearest-neighbor sites. The terms with coupling constant J_2 describe the orientation-dependent interaction between a surfactant molecule and a neighboring water molecule. This is the simplest form of such an interaction, assumed to be linear in the surfactant orientation $\hat{s}_u$. This interaction expresses the amphiphillic nature of a surfactant molecule, since a positive value of J_2 favors a surfactant orientation with its head pointing toward a neighboring water molecule. The last term gives the chemical potential energy of the surfactant molecules. This is consistent with analyzing the system in the grand canonical ensemble, where the surfactant concentration is controlled by the surfactant chemical potential μ_s, rather than in the canonical ensemble where the surfactant concentration is fixed.

In this work, the energy will be scaled with respect to J_1. Hence J_1 is replaced by 1 and J_2 by $j=J_2/J_1$. We define the scaled Hamiltonian, temperature, and chemical potential as $\hat{H}/J_1$, $t=k_BT/J_1$ and $\mu=\mu_s/J_1$. In terms of these scaled variables, Eq. (1) becomes

$$\hat{H}=-\sum_{\langle uv\rangle}\left[\sigma_u\sigma_v+j(\sigma_v\hat{s}_u\cdot\hat{r}_{uv}+\sigma_u\hat{s}_v\cdot\hat{r}_{vu})\right]$$

$$-\mu\sum_u(1-\sigma_u). \tag{2}$$

III. ZERO-TEMPERATURE AND LOW-TEMPERATURE ANALYSES

One advantage of a lattice model is that it can be analyzed by a variety of methods such as the mean-field and Bethe approximations [13], or by the low- and high-temperature expansion methods. The renormalization group approach and Monte Carlo methods can also be employed. In this paper the low-temperature expansion method is used. Due to the fact there is no explicit surfactant-surfactant interaction in our

model, it is possible to include exactly orientational fluctuations of surfactants in an expansion about the ground state of a phase. On the other hand, the inclusion of fluctuations that alter the ground-state concentration of a phase cannot be easily included in such an expansion. However, computer simulation results which are to be presented in a subsequent paper show that even at temperatures as high as $t\sim 1$ the concentration of an ordered phase deviates only slightly from the ground state, indicating that orientational fluctuations are the dominant mode of excitations at low temperature. This means that a low-temperature analysis that considers only this mode of excitation can obtain phase diagrams that include all the stable phases as well as correctly describe the qualitative behavior of the system.

First consider the water-rich (W) phase, which in the ground state consists of all sites being occupied by water. Since each site has 12 nearest neighbors, the zero-temperature grand canonical potential per site of the W phase (equal to the ground-state energy per site) is easily calculated to be

$$\frac{\Omega_W^0}{N} = -6, \tag{3}$$

where N is the number of sites in the lattice. On increasing the surfactant concentration, which in our model corresponds to increasing the chemical potential μ, it is expected that the micellar cubic (Q'') phase becomes stable. This consists of finite micelles arranged in a three-dimensional periodic array. The optimum size and shape of these micelles, however, are not certain *a priori*. The simplest possibility is a spherical micelle consisting of a central surfactant site and its 12 nearest neighbors. Computer simulation results found that at low temperature and at a chemical potential where the system is in a disordered micellar W phase, most of the observed micelles are indeed spherical or a slight distortion of it. In the ground state, the 12 surface surfactants orient themselves directly away from the central site, resulting in a water-surfactant interaction energy of $-3j$ per surface surfactant, which is the lowest possible water-surfactant interaction energy for a surfactant site in our model. Since in this model there are no explicit surfactant-surfactant interactions, the central surfactant has an interaction energy of zero. This means that a spherical micelle placed in the mixture in the ground-state W configuration, changes the energy by $\triangle E = -36j - 13\mu + 120$, where the final term of 120 is the water-water interaction due to the 13 sites before the addition of the micelle. For $\triangle E < 0$ or $\mu > (120 - 36j)/13$, the introduction of a micelle lowers the grand potential of the system, and hence a Q'' phase that consists of an ordered arrangement [18] which maximizes the concentration of these micelles is stable compared to the W phase. However, it is found that the Q'' phase is never stable when compared to other ordered phases such as the H or L_α phase, and therefore we go on to examine the latter.

The H phase consists of infinite cylindrical micelles in a periodic two-dimensional (2D) array. Figure 1 shows a two-dimensional slice through the H phase on the fcc lattice, which is represented as a stack of two-dimensional triangular lattices. The cross sections of the infinite micelles (open circles) are arranged in a 2D hexagonal array, where the distance between the centers of two neighboring cross sections is three lattice spacings. In the figure, the filled circles indicate water sites, and the open circles denote surfactant sites in a particular kth plane, while the squares and triangles about one of the micelles indicate the locations of surfactant sites of the micelle in the $(k+1)$th and $(k-1)$th planes, respectively. The arrows in one of the cells indicate the ground-state orientations of four surfactants in the kth plane. The two surfactants with the normal arrowheads orient themselves directly at two water sites in the same plane, whereas the surfactants with the filled and open arrowheads orient themselves directly at water sites in the $(k+1)$th and $(k-1)$th planes, respectively. The fact that the cross sections of the micelles are not circular is a consequence of the lattice structure. However, several systems exhibit intermediate I phases, which are cylindrical phases as is the H phase, but in which the cylinders have noncircular cross sections organized in rectangular, quadratic or monoclinic symmetry [19]. Since the phase shown in Fig. 1 has hexagonal symmetry, it is still appropriate to call this an H phase. Inspection of Fig. 1 shows that each plane of this phase can be spanned by unit cells of nine sites, of which four are surfactants and five are water, which implies that the surfactant concentration of this phase is $\frac{4}{9}$. The zero-temperature grand potential per site is

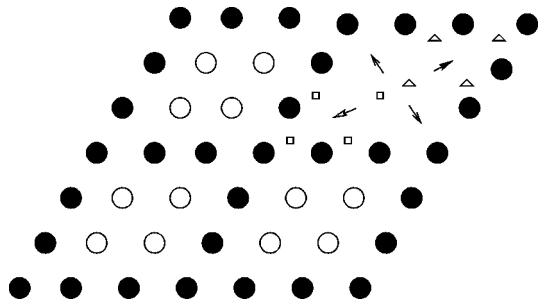

FIG. 1. Two-dimensional slice through the H phase on a fcc lattice, where the open and closed symbols denote surfactants and water molecules, respectively. The arrows in one of the cells indicate the ground state orientations of the surfactants.

$$\frac{\Omega_H^0}{N} = -\frac{16}{9} - \frac{4j}{3} - \frac{4\mu}{9}. \tag{4}$$

At nonzero temperature, the system is allowed to occupy higher energy configurations. If the temperature is very low, only configurations whose energies deviate slightly from the ground state are likely to occur. For the H phase, these are configurations where the surfactant molecules in the cylindrical micelles have orientations which differ from the ground-state orientations. Due to the absence of explicit surfactant-surfactant interactions, the orientational fluctuations of each surfactant are independent and can easily be summed. This produces a low-temperature expansion of the grand potential about the H ground state, given by

$$\frac{\Omega_H}{N} = \frac{\Omega_H^0}{N} - \frac{4t}{9}\ln(F_H), \tag{5}$$

where

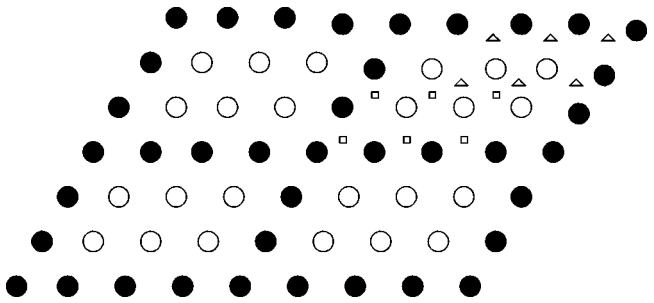

FIG. 2. Two-dimensional slice through the I phase on a fcc lattice.

$$F_H = 1 + 4\ \exp\left(\frac{-3j}{2t}\right) + 2\exp\left(\frac{-3j}{t}\right) + 4\exp\left(\frac{-9j}{2t}\right) + \exp\left(\frac{-6j}{t}\right)$$

is due to orientation fluctuations of the surfactant molecules.

Computer simulations of the model have indicated the occurrence of another cylindrical phase which consists of a 2D arrangement of infinite cylindrical micelles where each micelle has a rectangular cross section containing six surfactants. This phase is shown in Fig. 2, where the various symbols have the same meaning as before. For simplicity, arrows indicating surfactant orientations are omitted. Since the arrangement is rectangular, it is appropriate to call this the I phase. Analysis shows that this phase has a surfactant concentration of $\frac{1}{2}$, and a zero-temperature grand potential per site of

$$\frac{\Omega_I^0}{N} = -\frac{3}{2} - \frac{4j}{3} - \frac{\mu}{2}. \tag{6}$$

A low-temperature expansion about the ground state gives a grand potential of

$$\frac{\Omega_I}{N} = \frac{\Omega_I^0}{N} - \frac{t}{6}\ln 4 - \frac{t}{3}\ln F_H - \frac{t}{6}\ln\left[1 + \exp\left(\frac{-2j}{t}\right) + \exp\left(\frac{-4j}{t}\right)\right]. \tag{7}$$

The second term in Eq. (7) is due to the ground-state degeneracy of two of the surfactants in the cross section. The final two terms arise from allowing all the surfactant sites to have orientational fluctuations. At low temperature, the ground-state degeneracy term provides the most significant correction to the ground-state grand potential. Later, it will be shown that at $t=0$ the I phase is never stable compared to the H and L_α phases. However, due to the ground-state degeneracy, the I phase does become stable at nonzero temperature for large values of j.

Consider next the lamellar (L_α) phase, which is a stack of infinite surfactant bilayers. The phase is easily constructed in the stacked triangular lattice representation of the fcc lattice by alternating two surfactant layers with one water layer. Figure 3 pictures a two-dimensional slice through a lamellar phase showing alternating water monolayers and surfactant bilayers. This configuration is the most favorable one for strong surfactants (large j), since each water monolayer is in contact with two surfactant bilayers. Since the orientations of the surfactants are such that their heads reside on the surface of the bilayer, this configuration has the maximum possible number of surfactant head-water contacts. For weaker surfactants, lamellar phases with more than one layer of water sites between surfactant bilayers can also be stable, as is indicated by Monte Carlo simulations of the model discussed in Sec. IV.

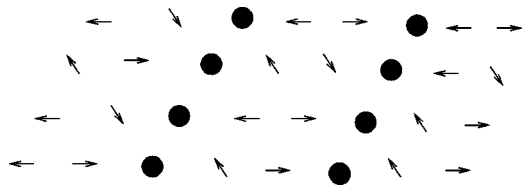

FIG. 3. Cross-sectional view of a lamellar (L_α) phase showing water monolayers alternating with surfactant bilayers. In the figure, filled circles are water molecules, and the arrows denote surfactant molecules with orientations in the direction of the arrows.

At zero temperature, for any value of j, only the lamellar phase with one water layer between surfactant bilayers is stable. This lamellar configuration has a surfactant concentration of $\frac{2}{3}$ and a grand potential per site of

$$\frac{\Omega_{L_\alpha}^0}{N} = -1 - \frac{4j}{3} - \frac{2\mu}{3}. \tag{8}$$

Ground-state analysis shows that each surfactant can orient itself toward any one of the three nearest neighbor water sites in the adjacent water monolayer. This degeneracy is partially indicated in Fig. 3. A low-temperature expansion of the grand potential that allows for orientational fluctuations of sites occupied by surfactant molecules gives

$$\frac{\Omega_{L_\alpha}}{N} = \frac{\Omega_{L_\alpha}^0}{N} - \frac{2t}{3}\ln 3 - \frac{2t}{3}\ln\left[1 + 2\ \exp\left(\frac{-2j}{t}\right) + \exp\left(\frac{-4j}{t}\right)\right]. \tag{9}$$

The second term in the expansion is due to the ground-state orientational degeneracy, while the final term is due to orientational fluctuations. At low temperature, the ground-state degeneracy gives the largest correction to the grand potential. At higher temperature, fluctuations become important, and the lamellar phase can assume configurations that are very different from the ground-state configuration. Aside from surfactant orientational fluctuations, two other modes of fluctuations may also be important. One mode is of fluctuations that bend the surfactant bilayers. However, in the present model, bilayer curvature fluctuations have a low probability of occurring. This is because on a fcc lattice, a bilayer can only bend at an angle of 60°. Furthermore, a bend in a single bilayer induces a bend in all bilayers, and so this mode of fluctuation causes a significant increase in energy. A more likely mode of fluctuations is one where the bilayers are pierced by water-filled channels.

Figure 4(a) shows a surfactant bilayer with a pinhole defect. The pinhole defect is the smallest possible water-filled

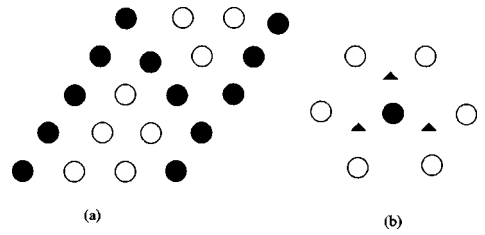

FIG. 4. Pinhole defect in a surfactant bilayer: (a) a side view of the defect; (b) a top view where the water is the filled circle and the open circles are surfactants. The triangles indicate the three possible locations of the other water site in the adjacent surfactant monolayer.

channel that can form in a bilayer, and consists of two water sites. Figure 4(b) shows a top view of the defect, where the three triangles indicate the possible locations of the other water site in the surfactant monolayer below. To minimize the free energy, the surfactants surrounding the channel orient themselves at an angle of 60° with the water-filled sites. At zero temperature, the placement of a pinhole changes the grand potential by $\triangle E=2\mu-7$. The result is rather curious, since the defect energy does not depend on the water-surfactant interaction parameter j. This result is exclusive to pinhole defects, since in general defect energies of larger water-filled channels depend on j. If $\triangle E<0$, which occurs when $\mu<3.5$, then the pinhole lowers the free energy, in which case an ordered 2D arrangement which maximizes the number of pinholes is more stable than a lamellar phase with no water channels. This is the catenoid lamellar (CL) phase which has been investigated recently by several authors [20–22]. This phase is only stable if the lamellar phase is already stable when compared to other phases. In the ground state, for $j>2$ and $\mu<3.5$ there is always a range of μ that increases with j where the CL phase is stable compared to the W phase. For this thermodynamic range, however, the lamellar phase is less stable than the H phase, and so the catenoid lamellar phase is never stable in our model. However, as will be discussed in Sec. IV, at nonzero temperature, water channels are observed to form in a stable lamellar phase for $\mu<3.5$, but their arrangement is disordered.

The surfactant-rich region of the phase diagram, which occurs at high μ, is populated by the inverse IQ', IH, IQ'', and S phases. Consider first the inverse bicontinuous cubic (IQ') phase, which is the inverse analog of the Q' phase. The bicontinuous cubic phase is a cubic arrangement of two nonintersecting infinite labyrinths of surfactant molecules separated by a single water film. For the inverse bicontinuous cubic phase, the roles of the water and surfactant are interchanged, and the phase consists of two water labyrinths separated by a single surfactant bilayer film. It is now the consensus that this intriguing phase is characterized by infinite periodic minimal surfaces (IPMS's) [23,24]. A minimal surface is a surface having at each point a mean curvature of zero. For binary mixtures of water and surfactants, the simplest example of an *infinite minimal surface* is the surfactant bilayer in a lamellar phase, which can be considered as an infinite volume that divides two nonintersecting infinite subvolumes (the two adjacent water layers). In this case the periodicity is one dimensional, but in general an IPMS can have three-dimensional periodicity. For a bicontinuous cubic

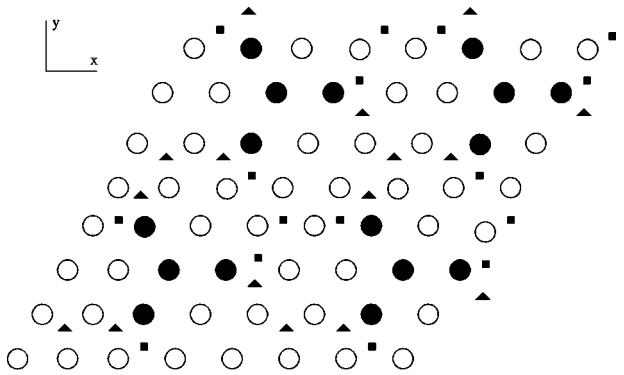

FIG. 5. Two-dimensional slice of the inverse bicontinuous cubic (IQ') phase. The symbols are explained in the text. The x and y axes of the Cartesian coordinate system are shown in the top left hand corner, with the z axis pointing out of the page.

(inverse bicontinuous cubic) phase, the minimal surface is located at the center of the water (surfactant bilayer) film that separates the two surfactant (water) labyrinths. For water-surfactant binary mixtures, the most commonly observed Q' (IQ') phase is the gyroid (G) phase with a space group $Ia3d$ [24]. A second type of IPMS phase called the diamond (D) phase with a space group $Pn3m$ has been identified [24]. A third possible IPMS is the so-called Schwarz *primitive* (P) surface with a space group $Im3m$, but the occurrence of this phase in water-surfactant binary mixtures has not been clearly established [24].

In this work, we were not successful in finding a stable Q' phase, but a stable IQ' phase has been identified. A two-dimensional slice of the phase is shown in Fig. 5. In the figure the open circles are surfactant sites in the kth plane and the filled circles, squares, and triangles are water sites in the kth, $(k+1)$th, and $(k-1)$th planes, respectively. Inspection of the structure reveals that the phase is bicontinuous. The water sites form an infinite three-dimensional network of rods joined coplanarly 3×3 with a body-centered-cubic (bcc) arrangement. To see that the water labyrinth forms a bcc array, assume that the center of a unit cell is located at any water site, and then the centers of the eight nearest neighbor cells are at the water sites located at $\pm[2\hat{x}+(2/\sqrt{3})\hat{y}+\sqrt{\frac{2}{3}}\hat{z}]$, $\pm[-2\hat{x}+(2/\sqrt{3})\hat{y}+\sqrt{\frac{2}{3}}\hat{z}]$, $\pm[(4/\sqrt{3})\hat{y}-\sqrt{\frac{2}{3}}\hat{z}]$, and $\pm3\sqrt{\frac{2}{3}}\hat{z}$, in a Cartesian coordinate representation with distance in units of one fcc lattice spacing. Simple algebra shows that the centers of the eight nearest neighbor unit cells are located at the corners of a cube with edge length of $2\sqrt{2}$. The labyrinth is in a class of structures called three-dimensional nets which was studied by Wells [25]. It is a uniform 3-connected net with the notation (10,3)-a [26] and a space group $I4_132$. This phase is very similar to the inverse G phase, since it is well known that the latter also possesses bcc symmetry and consists of two nonintersecting water labyrinths in which each labyrinth consists of water rods joined coplanarly 3×3 [24]. Indeed, Luzzati and Spegt [27] point out that the gyroid phase is one of the structures studied by Wells [25]. The main difference between the IQ' phase in our model and the inverse G phase observed in experiments is that the former has only one water labyrinth. For the latter, the two labyrinths are enantimorphic (mirror

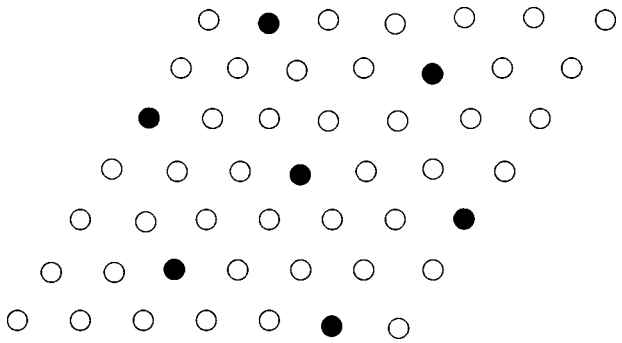

FIG. 6. Two-dimensional slice of the IH phase on a fcc lattice, where the open and closed circles are surfactants and water, respectively. The axes of the inverse cylindrical micelles make a 60° angle with the 2D plane.

images) resulting in an overall space group of $Ia3d$ [28,29]. The absence of a second labyrinth in our IQ' phase is probably due to the lattice constraint and the assumption in our model that a water molecule occupies the same volume as a surfactant molecule.

The surfactant concentration of the IQ' phase is $\frac{3}{4}$, which, as expected, is of an intermediate value between the L_α and IH phases. Due to the high symmetry of the phase, the ground-state grand potential per site is easily calculated to be

$$\frac{\Omega^0_{IQ'}}{N} = -\frac{3}{8} - \frac{3j}{2} - \frac{3\mu}{4}. \tag{10}$$

A low-temperature expansion that allows surfactant orientational fluctuations gives a grand potential of

$$\frac{\Omega_{IQ'}}{N} = \frac{\Omega^0_{IQ'}}{N} - \frac{t}{4}\ln F_{IQ'}, \tag{11}$$

where

$$F_{IQ'} = 1 + 4\exp\left(-\frac{j}{t}\right) + 2\exp\left(-\frac{2j}{t}\right) + 4\exp\left(-\frac{3j}{t}\right) + \exp\left(-\frac{4j}{t}\right).$$

Consider now the IH phase, which is the inverse analog of the hexagonal phase. The IH phase is made up of inverse cylindrical micelles, which are lines of water molecules surrounded by surfactants. The inverse cylindrical micelles are arranged in a two-dimensional hexagonal array. A two-dimensional slice of the IH phase is shown in Fig. 6, where the axes of the cylinders make a 60° angle with the plane. The IH phase has a surfactant concentration of $\frac{6}{7}$ and a zero-temperature grand potential of

$$\frac{\Omega^0_{IH}}{N} = -\frac{1}{7} - \frac{8j}{7} - \frac{6\mu}{7}. \tag{12}$$

A low-temperature expansion of the grand potential that includes fluctuations of the surfactant orientations gives

$$\frac{\Omega_{IH}}{N} = \frac{\Omega^0_{IH}}{N} - \frac{4t}{7}\ln 2 - \frac{4t}{7}\ln F_{IH1} - \frac{2t}{7}\ln F_{IH2}, \tag{13}$$

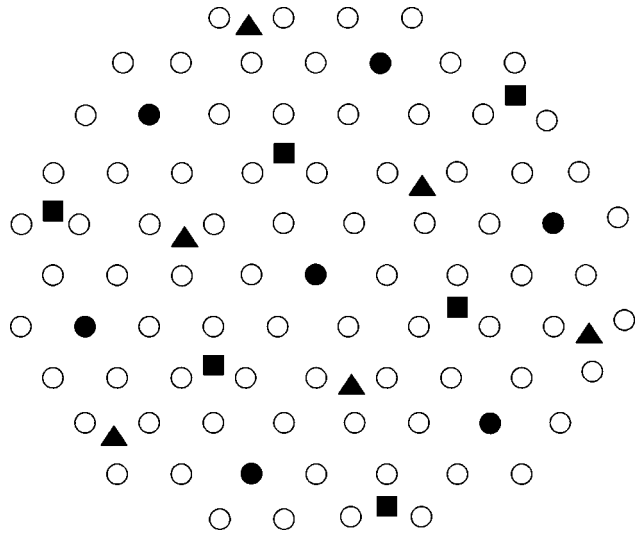

FIG. 7. The inverse cubic IQ'' phase on a fcc lattice, where a filled circle indicates the center of an inverse micelle, and the open circles indicate the surrounding surfactants in the kth plane. The squares and triangles indicate inverse micelle centers in the $(k+1)$th and $(k-1)$th plane, respectively.

where

$$F_{IH1} = 1 + \frac{1}{2}\exp\left(\frac{-j}{2t}\right) + \exp\left(\frac{-j}{t}\right) + \exp\left(\frac{-3j}{2t}\right) + \exp\left(\frac{-2j}{t}\right) + \frac{1}{2}\exp\left(\frac{-5j}{2t}\right) + \exp\left(\frac{-3j}{t}\right)$$

and

$$F_{IH2} = 1 + 4\exp\left(\frac{-j}{2t}\right) + 2\exp\left(\frac{-j}{t}\right) + 4\exp\left(\frac{-3j}{2t}\right) + \exp\left(\frac{-2j}{t}\right).$$

The second term in Eq. (13) is due to ground-state degeneracy, and constitutes the largest correction to the zero-temperature grand potential, while the final two terms arise from the surfactant orientational fluctuations.

Figure 7 shows the ground-state configuration of an inverse micellar cubic (IQ'') phase which is a distorted simple cubic arrangement of inverse micelles. An inverse micelle consists of a single water molecule surrounded by 12 nearest neighbor surfactant molecules that orient themselves directly toward the water molecule. Since each micelle consists of 13 molecules, and has a water-surfactant interaction energy of $-12j$, the zero-temperature grand potential is

$$\frac{\Omega^0_{IQ''}}{N} = -\frac{12j}{13} - \frac{12\mu}{13}. \tag{14}$$

A low-temperature expansion of the grand potential gives

$$\frac{\Omega_{IQ''}}{N} = \frac{\Omega^0_{IQ''}}{N} - \frac{t}{13}\ln\left[F^{12}_{IH2} + 12^{13}\exp\left(\frac{\mu - 12j}{t}\right)\right]. \tag{15}$$

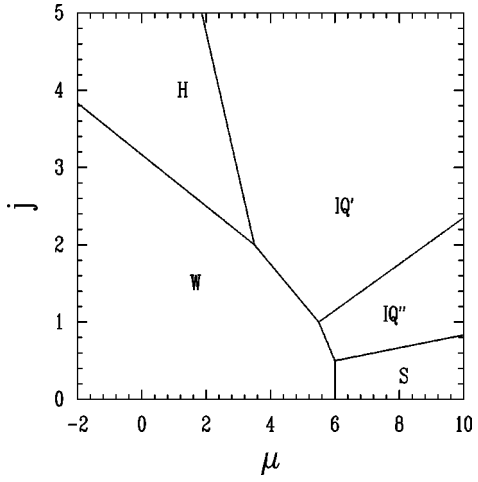

FIG. 8. Zero-temperature phase diagram.

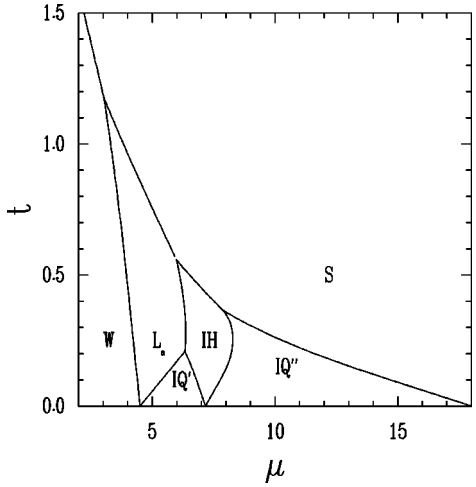

FIG. 9. Temperature (t) vs chemical potential (μ) phase diagram for interaction parameter $j=1.5$.

In Eq. (15) the first term in the argument of the logarithm includes all orientational configurations of the 12 surfactant sites surrounding a water molecule. In addition, for this phase, we have allowed for fluctuations that change the surfactant concentration. This is contained in the second term inside the logarithm, which arises from a water site being replaced by a surfactant. This fluctuation is included because it has a low excitation energy due to the high surfactant concentration of $\frac{12}{13}$.

Finally, at very high surfactant chemical potential the mixture is in a disordered surfactant-rich (S) phase. At zero temperature this consists of all sites in the lattice being occupied by surfactants. Since this phase has no interaction energy, the zero-temperature grand potential is simply

$$\frac{\Omega_S^0}{N}=-\mu. \tag{16}$$

At $t=0$, each surfactant site is allowed to assume all of its orientation states. This ground state degeneracy gives rise to a correction to the zero-temperature grand potential of

$$\frac{\Omega_S}{N}=-\mu-t\ \ln 12. \tag{17}$$

Employing the ground-state grand potentials given by Eqs. (3), (4), (6), (8), (10), (12), (14), and (16), a zero-temperature phase diagram shown in Fig. 8 is obtained by equating the grand potentials for all possible pairs of coexisting phases. In the phase diagram, for $j<0.5$ only the disordered W and S phases are stable. The IQ'' phase becomes stable for $j>0.5$, followed by the IQ' phase for $j>1$, and by the H phase for $j>2$. For $1<j<2$, at the W-IQ' phase boundary ($\mu=\frac{15}{2}-2j$), lamellar phases with any number of water layers between surfactant bilayers coexist with the W and IQ' phases. However, it is only along the W-IQ' phase boundary that the lamellar phase is stable, as elsewhere it is preempted by either the W phase or the IQ' phase as shown in Fig. 8. This is unexpected since the lamellar phase is the most commonly observed phase in computer simulations of the model [17]. On the other hand, the IQ' phase is observed in simulation only for large values of j and at low temperature [17]. This is because the L_α phase has a large ground-state degeneracy, whereas the IQ' phase has none, and thus at nonzero temperature the L_α phase quickly preempts the IQ' phase. At the zero-temperature IQ'-IQ'' phase boundary [$\mu=(13+20j)/6$], the IH phase is also stable. At $j=2$ and $\mu=3.5$, the H, W, and IQ' phases, as well as the previously discussed catenoid lamellar phase, all coexist. However, the CL phase is not stable at any other point on the phase diagram. The I phase is not stable at zero temperature for any value of j, but becomes stable at nonzero temperature for sufficiently large j.

As is expected, with increasing surfactant-water interaction parameter j, a larger number of ordered phases become stable. The ground-state results suggest that to obtain a phase diagram that shows completely the rich polymorphism of a binary water-surfactant mixtures, a sufficiently large interaction parameter j must be employed. However, although phase diagrams obtained by employing smaller values of j have fewer stable phases, they do exhibit behaviors that are not observed for larger values of j. In view of the variation in the behavior of the system with changing interaction parameter j, the values $j=1.5$, 3.0, and 5.0 are employed in Sec. IV.

IV. PHASE DIAGRAMS AT $T>0$

In this section, temperature-chemical potential phase diagrams are presented. As at zero temperature, the phase boundaries are determined by equating the grand potentials of possible pairs of coexisting phases. In general, the resulting phase transitions are first order, which is consistent with the fact that the various phases have different symmetries. This is also in accord with experimental results. Figure 9 shows the phase diagram for the interaction parameter $j=1.5$. With increasing μ, the W, L_α, IQ', IH, IQ'', and S phases are stable. In general, the slopes of the phase boundaries are negative. This is because as μ increases, phases with higher surfactant concentrations and hence higher entropies become stable, and so with increasing temperature high-surfactant-concentration phases increase their thermodynamic ranges of stability at the expense of lower concentration phases. Two exceptions are the L_α-IQ' and IH-IQ''

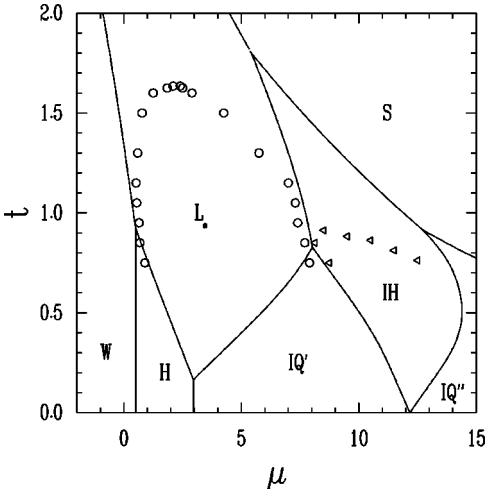

FIG. 10. Temperature (t) vs chemical potential (μ) phase diagram for interaction parameter $j=3.0$.

phase boundaries. In the former case, the L_α phase has a larger ground-state entropy than the IQ' phase, making the slope of the phase boundary positive. For the IH-IQ'' transition, the IH phase has a larger ground-state entropy than the IQ'' phase, which has none, making the initial slope of the phase boundary positive. However, at higher temperature the orientational entropy of the IQ'' phase becomes important, and the IQ'' phase range of stability expands making the slope of the phase boundary negative.

The L_α phase is stable up to $t=1.18$, above which only the disordered W and S phases are stable. Low-temperature analysis gives an expression of $\mu=6-t\ \ln 12$ for the W-S phase boundary, which in this approximation extends to $t=\infty$. However, it is expected that at high temperature, the W-S phase boundary should really end at a critical point. The mean-field and Bethe approximations give critical point values of $t=3$ and $\mu=6-3\ \ln 12=-1.455$, and $t=2.381$ and $\mu=-0.3141$ (for $j=1.5$), respectively. Better estimates can be obtained by the renormalization group or high-temperature expansion methods.

At $t=0$, the W-IQ'-L_α phase boundary obtained by equating Eqs. (3), (8), and (10) occurs at $\mu=\frac{15}{2}-2j$. In fact, along this phase boundary, lamellar phases with an arbitrary number of water layers between surfactant bilayers are equally stable. The low-temperature expansion method employed in this work found that these dilute lamellar phases are never stable at nonzero temperature. However, Monte Carlo simulation results to be presented in a subsequent paper have observed dilute lamellar phases for interaction parameter value $j=1.5$. In fact, a lamellar phase with surfactant number concentration as low as 0.07 has been observed to be stable. IQ', IH, and IQ'' are stable up to $t=0.21$, 0.56, and 0.37, respectively. Due to the fact that these phases are only stable at such low temperatures, they are not observed in computer simulation studies.

Figure 10 shows the phase diagram for the interaction parameter $j=3.0$. The phase diagram is qualitatively similar to the one for $j=1.5$, with the exception that the H phase is also stable. In addition to this, the thermodynamic range of stability of the ordered phases is much larger, with the L_α phase being stable up to a temperature of $t=4.7$. Although the W-S phase boundary is not visible in the figure, it does exist for $t>4.7$. However, since this boundary should really end in a critical point, it is likely that for $j=3$ the lamellar phase preempts the whole W-S coexistence line. For this value of j, Monte Carlo simulations have observed a stable IH phase as well as an L_α phase. The H, IQ', and IQ'' phases are not observed in simulations, although finite cylindrical micelles with cross sections identical to the infinite cylindrical micelles that make up the H phase (see Fig. 1) are observed in the disordered W phase. In Fig. 10 the circles and triangles indicate the L_α-disordered (either W or S) and IH-S phase boundaries, respectively, found by the Monte Carlo method. The simulations are performed only at temperatures above 0.75, since at lower temperature the Monte Carlo equilibration time becomes excessive. For temperatures below 1.2, the correlation between the W-L_α phase coexistence obtained by the Monte Carlo method and that obtained by the low-temperature expansion method is quite good. For the same temperature range and at higher μ, the S-L_α coexistence obtained by the Monte Carlo method lies close to the L_α-IH phase boundary obtained by low-temperature analyses. This suggests that in this thermodynamic range the disordered surfactant rich phase preempts the IH phase. At temperatures above 1.2, Monte Carlo data do not compare well with results obtained by low-temperature analyses. This is because the low-temperature analyses do not correctly calculate the grand potentials of the disordered W and S phases near the high-temperature coexistence boundaries with ordered phases. In these regions the W (S) phase is either disordered micellar (inverse micellar) or a sponge (L_3) phase. Due to their large entropies, low-temperature analyses of these phases are not expected to be accurate.

Only the lamellar phase with water monolayers alternating with surfactant bilayers is predicted to be stable by our low-temperature expansion. However, our Monte Carlo simulations [17] have observed the formation of water channels in surfactant bilayers. As discussed in Sec. III, for $j>2$ and at nonzero temperature, the dominant mode of fluctuations that destabilizes the one-dimensional order of the lamellar phase is the formation of water channels. It was shown that at $t=0$ and for $\mu>3.5$, the stable lamellar phase has a surfactant concentration of $\frac{2}{3}$. When the chemical potential is decreased below 3.5, the formation of water-filled pinholes in surfactant bilayers becomes energetically favorable and the surfactant concentration is decreased. Low-temperature analysis shows that the catenoid lamellar phase is never stable at nonzero temperature when compared to the H and L_α phases. This is because, although the addition of pinholes reduces the internal energy of the system, it also reduces the surfactant concentration which in turn reduces the entropy of the lamellar phase. However, for $\mu<3.5$ and $t>0$, the random formation of pinholes does occur in a stable lamellar phase [17]. For $\mu\sim 3.5$, the concentration of pinholes is small and the surfactant concentration of the lamellar phase is only slightly reduced from its maximum value of $\frac{2}{3}$. The concentration of pinholes increases with decreasing μ, reaching its maximum value near the H-L_α coexistence boundary, where there can be a significant reduction in the surfactant concentration. At higher temperature when the H phase is no longer stable and near the W-L_α

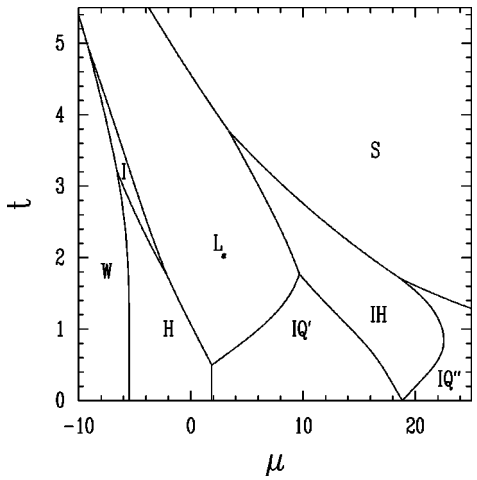

FIG. 11. Temperature (t) vs chemical potential (μ) phase diagram for interaction parameter $j=5.0$.

phase boundary, the formation of larger water channels becomes favorable, and the surfactant concentration is decreased even further until finally the order of the lamellar phase is destroyed. This behavior is not observed for $j<2$, where the formation of water channels in surfactant bilayers is never favorable; hence at high temperature and with decreasing μ the lamellar phase becomes more dilute by increasing the distance between surfactant bilayers.

The formation of water channels in surfactant bilayers of a lamellar phase has recently been investigated by several authors. Monte Carlo simulation studies [30] of the Larson lattice model have observed the formation of water channels in surfactant bilayers. More recently Netz and Schick [21] employed a self-consistent-field theory to investigate the stability of a lamellar phase perforated with hexagonally arranged water channels. Unexpectedly, they found that the water channels are hydrophobic, i.e., the surfactant molecules neighboring the water channels do not rearrange themselves to shield their tails from water. This is in contrast to a later Monte Carlo study by Muller and Schick [22], which found that the surfactants surrounding the channels do rearrange themselves in order to shield their tails from water, making the channels hydrophilic. In our model, the analysis of Sec. III found that the surfactants neighboring the pinholes tend to orient their head groups toward the water channels, which is consistent with hydrophilic channels. This is also the case for larger water channels for which Monte Carlo simulation has found the channels to be hydrophilic, which will be examined further in a subsequent [17] paper.

Figure 11 shows the phase diagram for the interaction parameter $j=5.0$. Qualitatively, the phase diagram is similar to the one for $j=3$, with the ordered phases being stable for a larger thermodynamic range. Formation of random water channels in surfactant bilayers also occurs for $\mu<3.5$ at nonzero temperature, as indicated by Monte Carlo simulation [17]. In addition to this, the intermediate I phase is also predicted by low-temperature analysis to be stable in a small thermodynamic range as indicated in Fig. 11. The I phase is also observed in Monte Carlo simulation for $j=5$. The H and IQ' phases as well as the L_α and IH phases are also observed in Monte Carlo simulations [17]. This is because, at such high j, the ordered phases are stable up to a much higher temperature than for lower values of j. The IQ'' phase is not observed in our simulations, even though Fig. 11 indicates that this phase is stable above $t\sim 1$, implying that the phase should be observable in Monte Carlo simulation. Of course, the low-temperature approximation may not be valid at this temperature since it does not take into account the entropic gain that results from the dispersion of finite inverse micelles when the IQ'' phase melts into the disordered S phase. For this reason, the IQ'' phase may in reality be stable only at temperatures much less than 1, making it unobservable by computer simulation.

V. CONCLUSION

In this paper, binary mixtures of water and surfactants are investigated using a simple Ising-like lattice model. The model extends the Ising model by giving a surfactant site a discrete set of orientations toward its nearest neighbors. It mimics the amphiphillic property of surfactants by making it energetically favorable for a surfactant molecule to orient itself toward water molecules. Although there are isotropic water-water and surfactant-surfactant interactions, the model does not include orientation-dependent anisotropic water-water and surfactant-surfactant interactions. Furthermore, it neglects the structure of surfactant molecules by assuming that these molecules are point particles. Despite this, the phase diagrams presented in Sec. IV exhibit a rich polymorphism. This suggests that the complex polymorphism observed in binary mixtures of water and surfactants is due mainly to their tendency to form water-surfactant interfaces. At a given temperature, the phase behavior is determined by the water-surfactant interfacial free energy as well as by the surfactant concentration (which in this model is controlled by μ). For $j>2$, cylindrical micelles (Fig. 1) are the most energetically favorable micelles, and hence the hexagonal phase is the first ordered phase to become stable as the concentration increases (increasing μ). At higher surfactant concentration, the lamellar phase becomes stable even though surfactant bilayers are not as energetically favorable as cylindrical micelles. This is because the amount of water-surfactant interface is maximized in the lamellar phase, making it stable in the surfactant concentration range between $\frac{1}{2}$ and $\frac{1}{3}$. Increasing the surfactant concentration further, the inverse IQ', IH, and IQ'' phases become stable to accommodate the high number of surfactant molecules. This behavior agrees with experimentally observed phase sequences.

The stability of the IQ' phase between the L_α and IH phase is significant, since inverse bicontinuous cubic phases are commonly observed in experimental studies of water-amphiphile mixtures [24]. Despite the lattice constraint of our model, there is a striking similarity between the IQ' and gyroid phases, suggesting that the gyroid structure may be as universal a structure as the lamellar or the cylindrical. The low-temperature analyses of Sec. III show that the IQ' phase has the lowest ground-state water-surfactant interaction per site ($-3j/2$), resulting in a large range of stability in the zero-temperature phase diagram (Fig. 8). However, the fact that the phase does not possess a ground-state entropy results in its small thermodynamic range of stability in the t-μ phase diagram (Figs. 9, 10, and 11). For this reason the IQ' phase is only observed in Monte Carlo simulation for high j.

The micellar and normal bicontinuous cubic phases are not stable in our model. Since in this model, infinite cylindrical micelles are more energetically favorable than finite micelles at low surfactant concentration, it is not surprising that the micellar cubic phase is not stable. Also it is noteworthy that for $j>2$ water channels tend to form in surfactant bilayers of a stable lamellar phase. As discussed earlier, in binary mixtures containing surfactants with very long alkyl tails, the intermediate phase between the H and L_α phases is usually not the Q' phase but a lamellar phase with water channel defects in surfactant bilayers. The defects can have two- or three-dimensional order, or be randomly dispersed in the bilayers [3]. This suggests that, in our model, the absence of the Q' phase is compensated for by the presence of the intermediate defective lamellar phase.

Another interesting result is the fact that both inverse and noninverse phases are stable in our model. This is contrary to most experimental observations in which either inverse phases or noninverse phases—but not both—are observed. As discussed in Sec. I, this behavior is due to steric interactions between surfactant tail groups which favor inverse phases when the tail-tail interactions supersede the head group repulsions. Since our model considers surfactants to be point particles, there are no anisotropic tail-tail interactions, and hence inverse phases occur naturally at high surfactant concentration (high μ).

As mentioned earlier, the low-temperature analyses employed in this work assume that the ordered phases retain their ground-state concentration and positional structure, while allowing orientational fluctuations of the surfactant sites. This approximation is justified by Monte Carlo simulation findings in which fluctuations that change the surfactant concentration or the positional structure of an ordered phase are rarely observed. In view of this, the phase diagrams obtained by this method should be quite accurate, especially at low temperature ($t<1$). However, at higher temperature, near the phase boundaries between ordered and disordered phases, concentration and structural fluctuations occur, and the approximation is probably less valid. For example, for the L_α-W phase transition at $j=1.5$ and $t>1$, Monte Carlo simulations show that the lamellar phase of concentration $\frac{2}{3}$ unbinds with decreasing μ to form a dilute lamellar phase of lower concentration before transforming into a disordered sponge phase. Similarly, for $j=5$ and at $t>1$, with decreasing μ and near the H-W phase boundary, computer simulations show that a stable H phase of concentration $\frac{4}{9}$ unbinds to form a lower-concentration phase of infinite cylindrical micelles that are not arranged in a two-dimensional array, before transforming into a disordered phase consisting of dispersed spherical micelles. A related point is the formation of water channels in surfactant bilayers of a stable lamellar phase for $j>2$. As discussed earlier, for these values of j and at low temperature, the formation of water-filled pinholes occurs for $\mu<3.5$. However, at higher temperature and for $\mu \ll 3.5$, Monte Carlo simulations indicate the formation of larger water channels which, with decreasing μ, results in melting of the lamellar phase into a disordered phase. These behaviors are not predicted by the simple low-temperature analyses, and are investigated by Monte Carlo methods to be presented in a subsequent paper [17].

ACKNOWLEDGMENTS

We wish to thank Professor B. G. Nickel and Professor M. J. Zuckermann for numerous discussions and helpful advice. This work was supported by the Natural Sciences and Engineering Research Council of Canada.

[1] R. R. Balmbra, J. R. Clunie, and J. F. Goodman, Nature (London) **222**, 1159 (1969).

[2] P. Sakya, J. M. Seddon, R. H. Templer, R. J. Mirkin, and G. J. T. Tiddy, Langmuir **13**, 3706 (1997); A. Gulik, H. Delacroix, G. Kirschner, and V. Luzzati, J. Phys. II **5**, 445 (1995); M. Clerc, *ibid.* **6**, 961 (1996).

[3] P. Kekicheff and G. J. T. Tiddy, J. Phys. Chem. **93**, 2520 (1989); J. Burgoyne, M. C. Holmes, and G. J. T. Tiddy, *ibid.* **99**, 6054 (1995).

[4] K. Larsson, J. Phys. Chem. **93**, 7304 (1989); D. C. Turner, Z.-G. Wang, S. M. Gruner, D. A. Mannock, and R. N. McElhaney, J. Phys. II **2**, 2039 (1992).

[5] H. Hasegawa, H. Tanaka, K. Yamasaki, and T. Hashimoto, Macromolecules **20**, 1651 (1987).

[6] K. I. Winey, E. L. Thomas, and L. J. Fetters, Macromolecules **25**, 2645 (1992).

[7] J. Charvolin and J. F. Sadoc, J. Phys. (Paris) **48**, 1559 (1987); **49**, 521 (1988); J. Phys. Chem. **92**, 5787 (1988); Physica A **176**, 138 (1991).

[8] G. Porte, J. Appell, P. Bassereau, J. Marignan, M. Skouri, I. Billard, and M. Delsanti, Physica A **176**, 168 (1991).

[9] G. Porte, in *Micelles, Membranes, Microemulsions, and Monolayers*, edited by W. M. Gelbart, A. Ben-Shaul, and D. Roux (Springer-Verlag, New York, 1994), p. 105.

[10] D. Roux, C. R. Safinya, and F. Nallet, in *Micelles, Membranes, Microemulsions, and Monolayers* (Ref. [9]), p. 303.

[11] G. Gompper and S. Klein, J. Phys. II **9**, 1725 (1992); G. Gompper and U. S. Schwarz, Z. Phys. B **B97**, 233 (1995).

[12] K. A. Dawson and J. Kurtovic, J. Chem. Phys. **92**, 5473 (1990).

[13] M. W. Matsen and D. E. Sullivan, Phys. Rev. A **41**, 2021 (1990); **46**, 1985 (1992); Phys. Rev. E **51**, 584 (1995).

[14] M. Laradji, H. Guo, M. Grant, and M. Zuckermann, Phys. Rev. A **44**, 8184 (1991); M. Laradji, H. Guo, and M. Zuckermann, J. Phys.: Condens. Matter **6**, 2799 (1994).

[15] A. Ciach and J. S. Høye, J. Chem. Phys. **90**, 1222 (1989); A. Ciach, J. S. Høye, and G. Stell, *ibid.* **95**, 5333 (1991); M. Skaf and G. Stell, *ibid.* **97**, 7699 (1992).

[16] R. G. Larson, J. Phys. II **6**, 1441 (1996).

[17] A. Linhananta and D. E. Sullivan (to be published).

[18] Although there are many possible arrangements of the Q'' phase, the most energetically favorable is a simple cubic arrangement with a surfactant concentration of 13/32.

[19] S. Alperine, Y. Hendrikx, and J. Charvolin, J. Phys. (France)

Lett. **46**, 27 (1985); P. Kekicheff and B. Cabane, J. Phys. (Paris) **48**, 1571 (1987).
[20] V. L. Golo, E. I. Kats, and G. Porte, Pis'ma Zh. Éksp. Teor. Fiz. **64**, 575 (1996) [JETP Lett. **64**, 630 (1996)].
[21] R. Netz and M. Schick, Phys. Rev. E **53**, 3875 (1996).
[22] M. Müller and M. Schick, J. Chem. Phys. **105**, 8282 (1996).
[23] L. E. Scriven, Nature (London) **263**, 123 (1976).
[24] V. Luzzati, R. Vargas, P. Mariani, A. Gulik, and H. Delacroix, J. Mol. Biol. **229**, 540 (1993); P. Mariani, V. Luzzati, and H. Delacroix, *ibid.* **204**, 165 (1988).
[25] A. F. Wells, *Three-Dimensional Nets and Polyhedra* (Wiley, New York, 1977).
[26] In the notation employed by Wells, an (n,p) net meets $p \times p$ at a vertex, and has a shortest circuit of n links. Seven (10,3) nets were studied by Wells, who indexed them by the letters *a* to *g*. The (10,3)-*a* net is 3-connected, and has all links of equal length, with all interbond angles of 120°.
[27] V. Luzzati and P. A. Spegt, Nature (London) **215**, 701 (1967).
[28] S. T. Hyde and S. Andersson, Z. Kristallogr. **168**, 213 (1984); W. Fischer and E. Koch, *ibid.* **179**, 31 (1987).
[29] The gyroid phase is unique among the known minimal surfaces. Most known minimal surfaces are spanned by linear nets which consist of twofold rotational axes embedded in the surfaces. The gyroid surface does not have a twofold rotational axis, and thus cannot be spanned by a linear net. Furthermore, the two labyrinths of most minimal surfaces are congruent, whereas in the gyroid surface they are oppositely congruent.
[30] R. G. Larson, J. Chem. Phys. **96**, 7904 (1992).